JURNAL KIMIA VALENSI
p-ISSN: 2460-6065; e-ISSN: 2548-3013
Journal homepage: https://journal.uinjkt.ac.id/index.php/valensi
Research Article

Unraveling the Influence of Type and Position Heteroatoms (N, O, S) on Asphaltene Aggregation Patterns

Mia Ledyastuti*, Intan Maulidhian Aribowo, Muhammad Fahri Afiki

Chemistry Department, Faculty of Mathematics and Natural Sciences, Institut Teknologi Bandung, Bandung 40132, Indonesia

Email: mia.ledyastuti@itb.ac.id

Article Info
Received: Feb 17, 2025
Revised: Apr 14, 2025
Accepted: Oct 7, 2025
Online: Dec 22, 2025

Citation:
Ledyastuti, M., Aribowo, I, M., & Afiki, M. F. (2025). Unraveling the Influence of Type and Position Heteroatoms (N, O, S) on Asphaltene Aggregation Patterns. *Jurnal Kimia Valensi*, 11(2), 291-299.

Doi: 10.15408/jkv.v11i2.44934

Abstract

Asphaltenes, the heaviest fraction in petroleum and coal, are composed of polycyclic aromatic hydrocarbons (PAHs) with aliphatic side chains and heteroatoms (N, O, S). Previous studies have shown that these heteroatoms have a significant influence asphaltene aggregation. This study investigates the impact of heteroatom position and type, as well as solvent, on asphaltene aggregation behavior by employing molecular dynamics simulations of modified CA21 asphaltene. Simulations were conducted using GROMACS 2024.3. Analysis of simulation trajectories revealed that in water, all asphaltene models exhibited asphaltene-asphaltene radial distribution functions (RDFs) below 1 nm, indicating predominantly parallel or parallel-offset π-π interactions. In contrast, asphaltenes with an oxygen heteroatom at the end of the aliphatic chain when dissolved in hexane and toluene solvents, displayed unique shape aggregation, attributed to hydrogen bonding between the terminal oxygen atoms. The presence of heteroatoms within the aliphatic chain generally slowed aggregation, with the observed order of aggregation rates being S > N > O.

Keywords: Asphaltene aggregation, heteroatom, hydrogen bonding, parallel offset, π-π interactions

1. INTRODUCTION

Asphaltene is the heaviest fraction found in petroleum and coal [1]. The structure of asphaltene consists of polyaromatic hydrocarbons, aliphatic side chains, and heteroatoms such as N, O, or S. Generally, asphaltene is defined based on its solubility: it is soluble in aromatic solvents but insoluble in n-alkanes [2]. Asphaltene can form aggregates and deposits due to interactions between aromatic rings in the molecule [3]. The dominant interaction in asphaltene is the π-π interaction. DFT calculations revealed that in the absence of water molecules, asphaltene molecules exhibit strong π-π interactions, and these interactions increase with an increasing number of aromatic rings within the asphaltene structure [4]. Additionally, aliphatic chains and heteroatoms in asphaltene can also contribute to aggregation through van der Waals and electrostatic interactions [5]. Heteroatoms can also interact with mineral surfaces during oil transportation, leading to adsorption at the oil-water interface. This phenomenon results in the formation of deposits that can disrupt oil transportation processes [6,7]. Asphaltene deposits can also damage oil transportation equipment such as pipelines, leading to high maintenance costs [8–10].Therefore, studying asphaltene aggregation is crucial to prevent these problems.

Previous studies have highlighted the significant influence of solvents and heteroatoms on asphaltene behavior. Gabrienko et al. (2015) found that asphaltenes with fewer heteroatoms are more stable than those rich in heteroatoms [11]. This is due to the different intermolecular forces present. Asphaltenes with oxygen heteroatoms are considered less stable, while those with pyrrole and pyridine groups have intermediate stability. Mizuhara et al. (2020) suggested that the heteroatom forms hydrogen bond with water molecules [12]. However, heteroatoms located on aromatic rings can enhance asphaltene aggregation. Bai et al. (2019) analyzed the influence of N, O, and S heteroatoms in asphaltenes on adsorption and desorption on silica surfaces [13]. They

found that the presence of carboxyl (COOH) groups increases electrostatic interaction energy. The interaction energy for asphaltenes with amino (NH_2) and thiol (SH) groups is lower [13]. Bai also found that heteroatoms located at the center of aromatic groups and in the middle of aliphatic chains can increase electrostatic energy, with the order NH > O > S, and heteroatoms in aliphatic chains having a greater effect than those in aromatic groups [13].

Based on previous studies, the strength of electrostatic interactions can be influenced by the increasing polarity of the substituted heteroatom. Additionally, sulfur atoms have been found to contribute more significantly to van der Waals interactions. In another study by Ramírez et al. (2021), it was found that asphaltene molecules containing heteroatoms have a higher tendency to form aggregates [14]. Asphaltene molecules with sulfur heteroatoms have the highest tendency. According to Ekramipooya et al. (2021), the presence of nitrogen in all positions (aromatic and aliphatic) can increase electrostatic interactions, while sulfur increases van der Waals interactions [15]. Heteroatoms located at the end of the molecule can form hydrogen bonds, thereby increasing the interaction energy. The presence of additional interactions, such as hydrogen bonding, decreases the solubility of asphaltene in hexane and toluene [15].

This study employed the CA21 asphaltene model, derived from Indonesian coal [16], to investigate its behavior in various solvents. The CA21 model was modified by incorporating alkyl chains and substituting specific carbon atoms with heteroatoms (N, O, and S) to explore the impact of these structural variations on asphaltene properties. The GROMACS software and the GROMOS 54A7 force field were used for the simulations, which were conducted at a temperature of 300 K and a pressure of 1 bar. The primary focus was to understand the influence of heteroatoms on the intermolecular interactions and dynamics of asphaltene molecules under different solvents.

2. RESEARCH METHODS

Asphaltene Models

Molecular models were generated based on the CA21 structure, derived from the characterization of a coal sample from Indonesia [16]. This initial aromatic structure was modified by incorporating alkyl chains and heteroatoms (N, O, S) at various positions, resulting in twelve distinct models: N1, N2, N3, N4, O1, O2, O3, O4, S1, S2, S3, and S4. For instance, model N1 signifies that a nitrogen heteroatom occupies position 1. The general structure of the asphaltene model is illustrated in **Figure 1**.

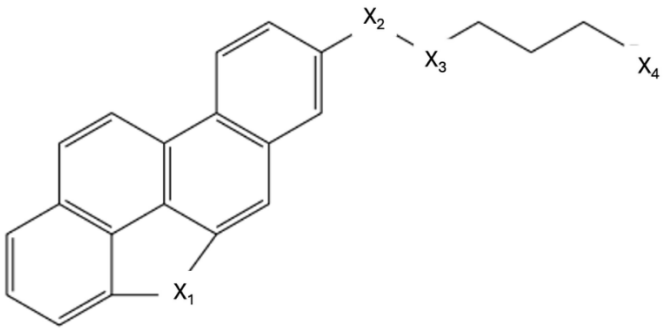

Figure 1. The general structure of asphaltene model. X1, X2, X3, and X4 respectively designate the heteroatom (X) located at positions 1, 2, 3, and 4.

The Avogadro software[17] was utilized to construct and manipulate these molecular structures, generating files in the .pdb format. Subsequently, the .pdb files were uploaded to the Automated Topology Builder (ATB) website [18]. ATB automatically generated the corresponding topology files (.itp) using the GROMOS 54a7 force field [19]. Finally, the .top files were created following the guidelines provided by the ATB website [18].

Molecular Dynamics Simulation

We employed a cubic simulation system with dimensions of 5x5x5 nm^3. Five identical asphaltene molecules were initially placed within the cubic box using the *gmx insert-molecules* command. Subsequently, the box was completely solvated with solvents utilizing the *gmx solvate* command. The solvents employed in this investigation were water, hexane, and toluene. The number and size of the asphaltene molecules present determined the number of solvent molecules incorporated within the simulation box.

Molecular dynamics simulations were conducted in three stages: energy minimization, equilibration, and production using GROMACS.2024.3 [20]. Energy minimization, employing the steepest descent algorithm with a maximum force limit of 1000 kJ/mol^{-1} nm^{-1}, was

performed for 50,000 steps to minimize the system's potential energy. Subsequently, equilibration was carried out in two phases: NVT equilibration (constant number of particles, volume, and temperature) for 100 ps and NPT equilibration (constant number of particles, pressure, and temperature) for 1100 ps, both utilizing the leap-frog integrator. The production phase, lasting 50 ns, employed periodic boundary conditions in all three dimensions, a 2.0 fs timestep, and the Particle Mesh Ewald (PME) method[21] for long-range electrostatic interactions. The LINCS algorithm[22] constrained bond lengths, while the V-rescale thermostat[23] and Parrinello-Rahman barostat[24] maintained temperature (300 K) and pressure (1 bar), respectively. Non-bonded interactions were handled with a 1.0 nm cutoff distance.

Trajectory Analysis

The analysis encompassed two key aspects: minimum distance calculations and Radial Distribution Function (RDF) analysis. Minimum distance calculations between asphaltene molecules were performed to confirm the presence of asphaltene aggregates within each simulated system. RDF analysis, utilizing the center of mass of one aromatic group on each asphaltene molecule as the reference point, was employed to investigate intermolecular interactions, including π-π interactions. The RDF in GROMACS was calculated using equation 1.

$$g_{AB} = \frac{\langle \rho_B(r) \rangle}{\langle \rho_B \rangle_{lokal}} \quad \ldots\ldots\ldots\ldots\ldots\ldots \quad (1)$$

Where $\langle \rho_B(r) \rangle$ represents the density of atom B at a distance r from atom A, and $\langle \rho_B \rangle_{lokal}$ is the average density of atom B in all shells surrounding atom A within a maximum distance of r_{max}.

Hydrogen bond interactions between asphaltene molecules were analyzed using the *gmx hbond-legacy* command. Hydrogen bonds were defined based on angular cutoff (hydrogen-donor-acceptor) and distance (hydrogen-acceptor) criteria. The default cutoffs for angle and distance in this command are 30 degrees and 0.35 nm, respectively.

3. RESULTS AND DISCUSSION

Visualizing the simulation trajectories revealed the aggregation of all asphaltene models in the water solvent. The presence of a single heteroatom in each model did not significantly alter the overall polarity of the asphaltene. Hydrophobic properties remained dominant in the simulated asphaltene models. In contrast, all asphaltene models demonstrated solubility in toluene. Interestingly, the behavior of asphaltene in hexane deviated from the conventional definition, which states that asphaltenes are insoluble in aliphatic solvents like hexane [2]. In our simulations, asphaltene displayed unstable aggregation behavior in hexane. **Figure 2** illustrates the behavior of the N1 model in various solvents at 300 K. While the snapshot at 50 ns showed no aggregation in hexane, an inset revealed a transient aggregation event at 2 ns.

Minimum distance calculations between asphaltene molecules further supported this observation. Aggregation was considered to occur when the intermolecular distance between asphaltene molecules fell below 0.3 nm [13]. **Figure 3** illustrates the distinct aggregation behaviors of asphaltenes in different solvents. In water, asphaltenes rapidly formed stable aggregates upon initiation of the simulation. Conversely, asphaltenes remained dispersed in toluene throughout the simulation, with no evidence of aggregation. In hexane, asphaltenes exhibited initial aggregation followed by a gradual dispersion phase, characterized by intermolecular distances consistently exceeding 0.3 nm.

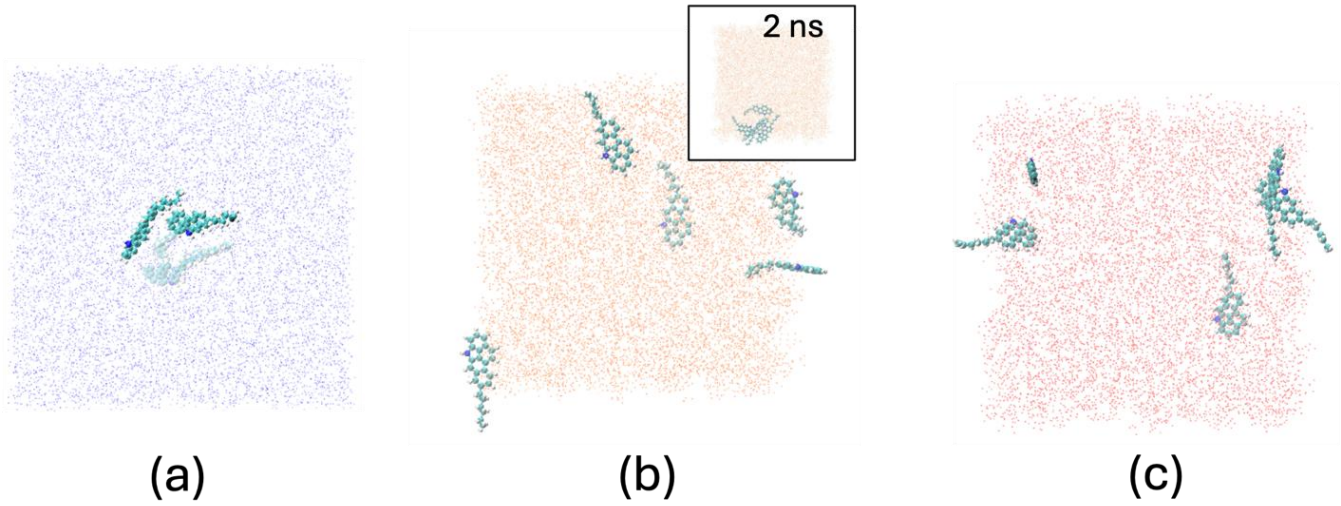

Figure 2. Snapshots model N1 at 50 ns of simulation time (300 K) in different solvent: (a) water, (b) hexane, and (c) toluene

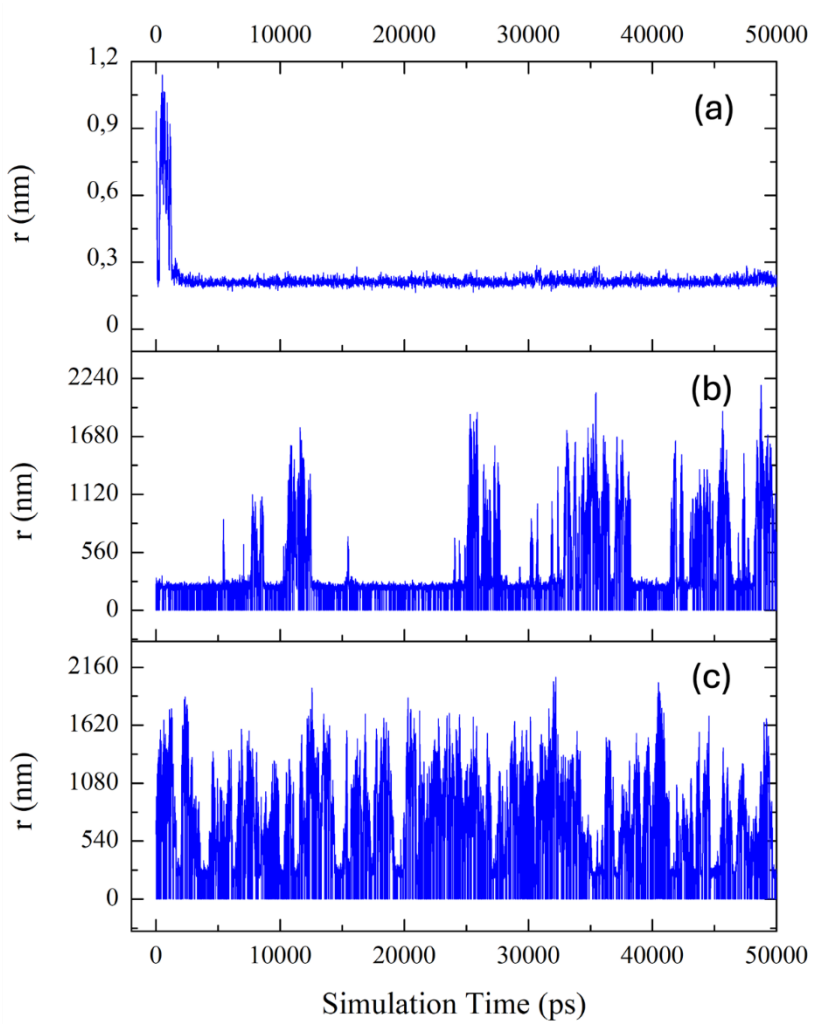

Figure 3. The evolution of minimum intermolecular distances of asphaltene model N1 at 300 K in different solvent: (a) water, (b) hexane, and (c) toluene

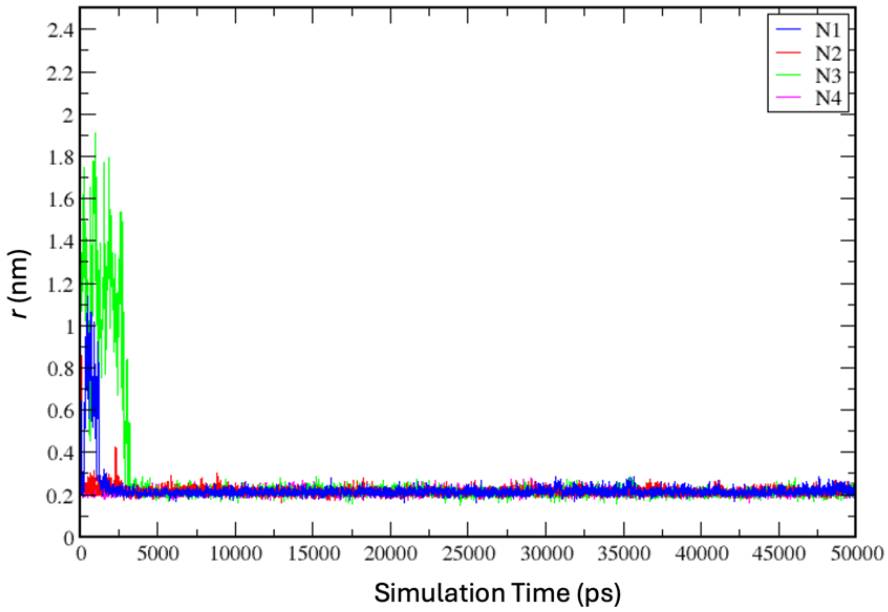

Figure 4. The aggregation time for asphaltene model with heteroatom N in various position (see **Figure 1**)

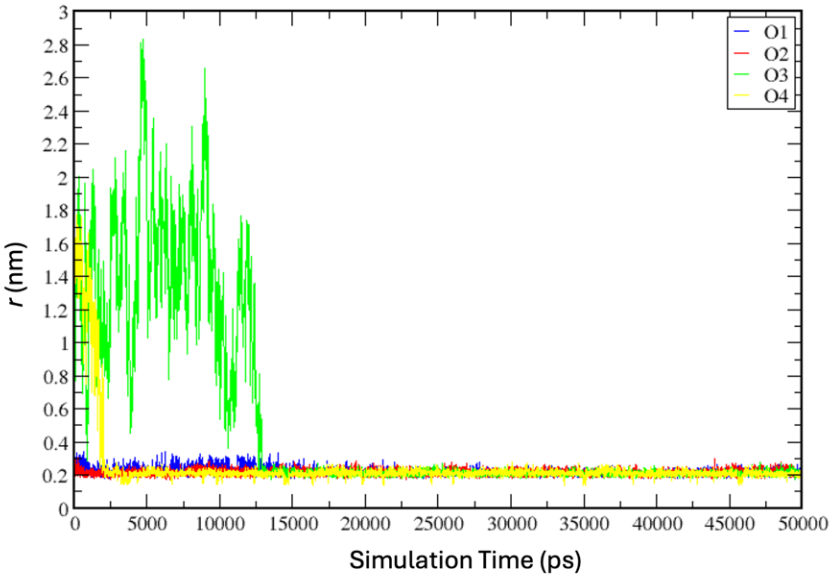

Figure 5. The aggregation time for asphaltene model with heteroatom O in various position (see **Figure 1**)

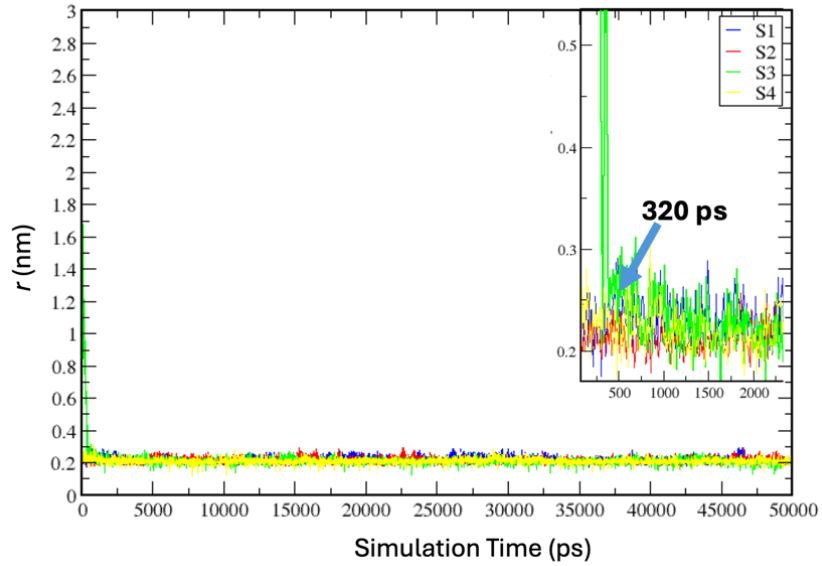

Figure 6. The aggregation time for asphaltene model with heteroatom O in various position (see **Figure 1**)

In aqueous environments, the position and type of heteroatoms significantly influenced asphaltene aggregation. Asphaltene models with heteroatoms at position 3 (N3, O3, and S3) exhibited slower aggregation kinetics compared to models with the same heteroatoms at other positions (**Figures 4-6)**. The observed order of aggregation propensity was S > N > O, consistent with previous findings by Ramírez et al. (2021), which indicated that sulfur-containing asphaltenes exhibit faster aggregation rates [14]. This slower aggregation for models with heteroatoms at position 3 (N3, O3, and S3) likely arises from weaker interactions within the aromatic regions. A more comprehensive understanding of these observations requires detailed electronic structure calculations for each model. Meanwhile, the presence of heteroatoms at positions 1, 2, and 4 did not show a significant impact on aggregation rate. The aggregation process occurred almost immediately after the simulation started, with asphaltene molecules approaching each other to a distance of less than 0.3 nm.

As shown in **Figure 2**, the observed aggregation is primarily driven by interactions in the aromatic regions, commonly referred to as π-π interactions. To confirm this, RDF analysis was conducted. The results in **Table 1** indicate that the peak for all asphaltene models in water falls within the distance (*r*) range of 0.38-0.95 nm. In this π-π interaction analysis, only asphaltene in water was considered due to its stable aggregation. Generally, all models except N2, N3, and N4 exhibited two peaks in the RDF analysis. N2, N3, and N4 showed only a single peak, while model S2 had three peaks. The number of peaks can indicate the types of interactions occurring within the system. The

peak with the highest value at a specific distance (*r*) indicates the most dominant interaction in the system. For all models except O2, the first peak was the highest.

π-π interactions in asphaltenes can exhibit three primary configurations: parallel, parallel-offset, and T-shaped [25]. The Dickie-Yen model[26] suggests that parallel configurations occur at distances of 0.35-0.38 nm, while other studies indicate parallel configurations at around 0.5 nm [27,28]. Parallel-offset and T-shaped configurations have been observed at distances around 1 nm, depending on the size of the asphaltene molecule [14]. Generally, the data in **Table 1** indicate that parallel and parallel-offset configurations dominate π-π interactions in asphaltene models with O and S heteroatoms. The N1 model likely exhibits both parallel-offset and T-shaped configurations, with parallel-offset being the dominant interaction. Model S2 exhibits a complete set of configurations with three peaks in its RDF.

In addition to π-π interactions, the presence of nitrogen (N) and oxygen (O) heteroatoms allows for the formation of hydrogen bonds. Models N1, N2, N3, N4, and O4 have the potential to form hydrogen bonds between asphaltene molecules. Hydrogen bond analysis revealed that models N1, N2, N3, and N4 exhibited only a single hydrogen bond in hexane, while model O4 displayed five hydrogen bonds (**Figure 7**). The same pattern was also observed in toluene. This suggests a higher propensity for hydrogen bond formation in model O4. Furthermore, the hydrogen bonds in model O4 appeared more stable compared to the fluctuating hydrogen bonds observed in models N1 to N4. This enhanced hydrogen bonding in model O4, likely attributed to the higher electronegativity of oxygen, contributed to the unique aggregation patterns observed in hexane and toluene, as shown in **Figure 8**. The circular pattern illustrated in **Figure 8** is due to hydrogen bonding between the oxygen atoms of one asphaltene and the electropositive hydrogen atoms of another asphaltene. The system formed a maximum of five hydrogen bonds, corresponding to the total number of asphaltene molecules present. Since hexane and toluene solvents lack electropositive hydrogen atoms, any electropositive hydrogen must come solely from the asphaltene. This explains the stability of this unique pattern throughout the simulation.

Table 1 RDF analysis of all asphaltene model in water

Model	Heteroatom Position	1st Peak		2nd Peak		3rd Peak	
		$g(r)$	$r(nm)$	$g(r)$	$r(nm)$	$g(r)$	$r(nm)$
N1	Aromatic	50.20	0.64	15.61	0.95	-	-
N2	Aliphatic	41.65	0.65	-	-	-	-
N3	Aliphatic	49.55	0.50	-	-	-	-
N4	Aliphatic	47.69	0.63	-	-	-	-
O1	Aromatic	54.55	0.38	18.12	0.82	-	-
O2	Aliphatic	31.36	0.50	35.71	0.70	-	-
O3	Aliphatic	29.64	0.51	27.88	0.71	-	-
O4	Aliphatic	47.59	0.51	41.57	0.72	-	-
S1	Aromatic	54.48	0.39	30.23	0.74	-	-
S2	Aliphatic	63.76	0.38	49.04	0.52	37.54	0.76
S3	Aliphatic	47.36	0.43	35.03	0.73	-	-
S4	Aliphatic	53.89	0.50	37.09	0.71	-	-

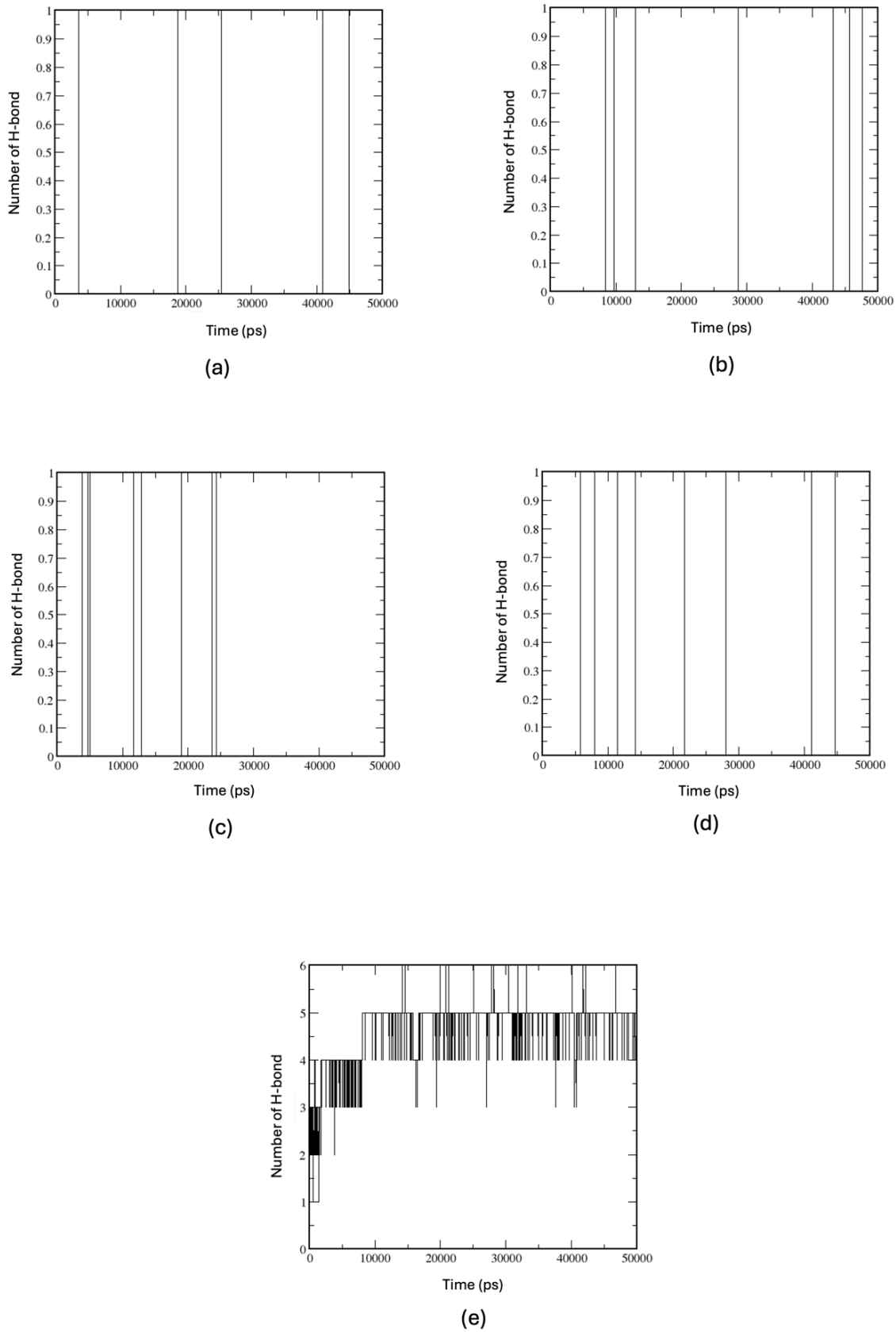

Figure 7. Hydrogen bond of asphaltene-asphaltene in hexane (a) N1, (b) N2, (c) N3, (d) N4 and (e) O4.

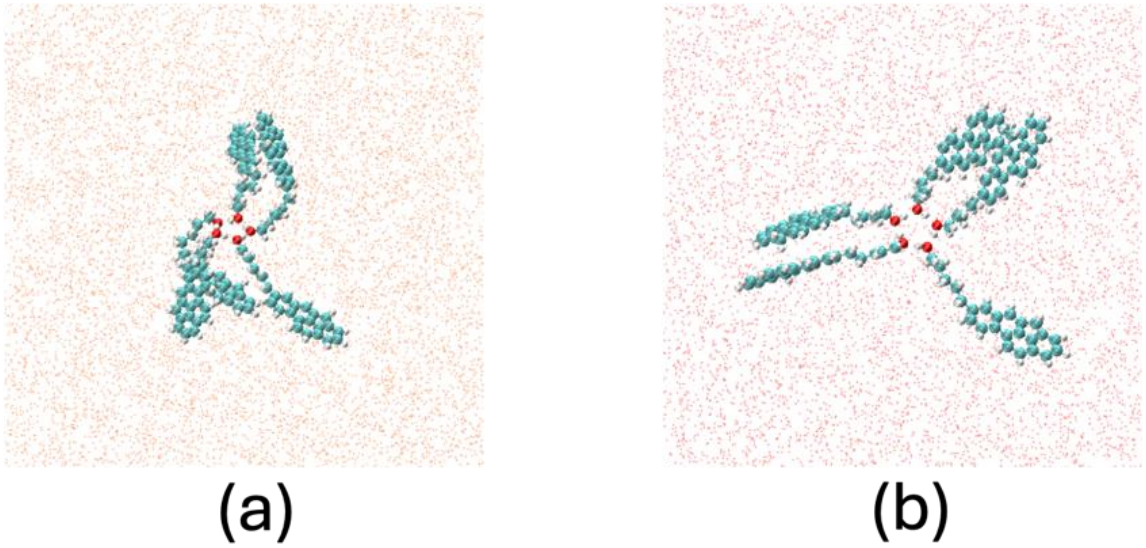

Figure 8. The different aggregate shape shown by model O4. (a) Snapshot O4 in hexane, (b) Snapshot O4 in toluene

4. CONCLUSIONS

Molecular dynamics simulations revealed that stable aggregation of the modified CA21 asphaltene was exclusively observed in aqueous environments. While aggregation of asphaltene in hexane is expected, our simulations demonstrated its solubility in this solvent. The position of heteroatoms significantly influenced the aggregation kinetics, with models N3, O3, and S3 exhibiting the slowest aggregation rates among their respective heteroatom groups. Model S3 exhibited the fastest aggregation rate, while O3 demonstrated the slowest. π-π interactions were identified as the dominant driving force for aggregation, primarily resulting in parallel and parallel-offset configurations. RDF analysis suggested that model N1 may exhibit T-shaped configurations in addition to parallel and parallel-offset arrangements. Hydrogen bonding also contributed to aggregation, particularly in model O4, leading to unique aggregation patterns observed in hexane and toluene. The enhanced hydrogen bonding observed in model O4 can be attributed to the higher electronegativity of oxygen compared to nitrogen, resulting in stronger hydrogen bonds in the O4 model. The findings of this study provide valuable insights into asphaltene aggregation mechanisms, paving the way for the development of more effective prevention strategies.

REFERENCES

1. Gharbi K, Benamara C, Benyounes K, Kelland MA. Toward Separation and Characterization of Asphaltene Acid and Base Fractions. *Energy & Fuels*. 2021;35(18):14610-14617. doi:10.1021/acs.energyfuels.1c01999
2. Yaseen S, Mansoori GA. Molecular dynamics studies of interaction between asphaltenes and solvents. *J Pet Sci Eng*. 2017;156:118-124. doi:10.1016/j.petrol.2017.05.018
3. *Essentials of Flow Assurance Solids in Oil and Gas Operations*. Elsevier; 2023. doi:10.1016/C2021-0-00361-8
4. Acevedo S, Castillo J. Asphaltenes: Aggregates in Terms of A1 and A2 or Island and Archipielago Structures. *ACS Omega*. 2023;8(5):4453-4471. doi:10.1021/acsomega.2c06362
5. Liu J, Zhao Y, Ren S. Molecular Dynamics Simulation of Self-Aggregation of Asphaltenes at an Oil/Water Interface: Formation and Destruction of the Asphaltene Protective Film. *Energy & Fuels*. 2015;29(2):1233-1242. doi:10.1021/ef5019737
6. He L, Lin F, Li X, Sui H, Xu Z. Interfcial sciences in unconventional petroleum production: from fundamentals to applications. *Chem Soc Rev*. 2015;44(15):5446-5494. doi:10.1039/C5CS00102A
7. Moud AA. Asphaltene induced changes in rheological properties: A review. *Fuel*. 2022;316:123372. doi:10.1016/j.fuel.2022.123372
8. Zhang J, Wei Q, Zhu B, et al. Asphaltene aggregation and deposition in pipeline: Insight from multiscale simulation. *Colloids Surf A Physicochem Eng Asp*. 2022;649:129394. doi:10.1016/j.colsurfa.2022.129394
9. Moncayo-Riascos I, De Leon J, Garcia-Martinez JA, Garcia-Cruz I, Lira-Galeana C. Multiscale simulation of asphaltene deposition in pipeline flows. *J Pet Sci Eng*. 2019;183:106376. doi:10.1016/j.petrol.2019.106376
10. Alhosani A, Daraboina N. Unified Model to Predict Asphaltene Deposition in Production

Pipelines. *Energy & Fuels*. 2020;34(2):1720-1727. doi:10.1021/acs.energyfuels.9b04287
11. Gabrienko AA, Morozov E V., Subramani V, Martyanov ON, Kazarian SG. Chemical Visualization of Asphaltenes Aggregation Processes Studied in Situ with ATR-FTIR Spectroscopic Imaging and NMR Imaging. *The Journal of Physical Chemistry C*. 2015;119(5):2646-2660. doi:10.1021/jp511891f
12. Mizuhara J, Liang Y, Masuda Y, Kobayashi K, Iwama H, Yonebayashi H. Evaluation of Asphaltene Adsorption Free Energy at the Oil–Water Interface: Role of Heteroatoms. *Energy & Fuels*. 2020;34(5):5267-5280. doi:10.1021/acs.energyfuels.9b03864
13. Bai Y, Sui H, Liu X, He L, Li X, Thormann E. Effects of the N, O, and S heteroatoms on the adsorption and desorption of asphaltenes on silica surface: A molecular dynamics simulation. *Fuel*. 2019;240:252-261. doi:10.1016/j.fuel.2018.11.135
14. Ramírez L, Moncayo-Riascos I, Cortés FB, Franco CA, Ribadeneira R. Molecular Dynamics Study of the Aggregation Behavior of Polycyclic Aromatic Hydrocarbon Molecules in *n* -Heptane–Toluene Mixtures: Assessing the Heteroatom Content Effect. *Energy & Fuels*. 2021;35(4):3119-3129. doi:10.1021/acs.energyfuels.0c04153
15. Ekramipooya A, Valadi FM, Farisabadi A, Gholami MR. Effect of the heteroatom presence in different positions of the model asphaltene structure on the self-aggregation: MD and DFT study. *J Mol Liq*. 2021;334:116109. doi:10.1016/j.molliq.2021.116109
16. Schuler B, Meyer G, Peña D, Mullins OC, Gross L. Unraveling the Molecular Structures of Asphaltenes by Atomic Force Microscopy. *J Am Chem Soc*. 2015;137(31):9870-9876. doi:10.1021/jacs.5b04056
17. Hanwell MD, Curtis DE, Lonie DC, Vandermeersch T, Zurek E, Hutchison GR. Avogadro: an advanced semantic chemical editor, visualization, and analysis platform. *J Cheminform*. 2012;4(1):17. doi:10.1186/1758-2946-4-17
18. Stroet M, Caron B, Visscher KM, Geerke DP, Malde AK, Mark AE. Automated Topology Builder Version 3.0: Prediction of Solvation Free Enthalpies in Water and Hexane. *J Chem Theory Comput*. 2018;14(11):5834-5845. doi:10.1021/acs.jctc.8b00768
19. Huang W, Lin Z, van Gunsteren WF. Validation of the GROMOS 54A7 Force Field with Respect to β-Peptide Folding. *J Chem Theory Comput*. 2011;7(5):1237-1243. doi:10.1021/ct100747y
20. Abraham MJ, Murtola T, Schulz R, et al. GROMACS: High performance molecular simulations through multi-level parallelism from laptops to supercomputers. *SoftwareX*. 2015;1-2:19-25. doi:10.1016/j.softx.2015.06.001
21. Darden T, York D, Pedersen L. Particle mesh Ewald: An $N \cdot \log(N)$ method for Ewald sums in large systems. *J Chem Phys*. 1993;98(12):10089-10092. doi:10.1063/1.464397
22. Hess B, Bekker H, Berendsen HJC, Fraaije JGEM. LINCS: A linear constraint solver for molecular simulations. Journal of Computational Chemistry. *J Comput Chem*. 1998;18(12):10089-10092.
23. Bussi G, Donadio D, Parrinello M. Canonical sampling through velocity rescaling. *J Chem Phys*. 2007;126(1). doi:10.1063/1.2408420
24. Parrinello M, Rahman A. Polymorphic transitions in single crystals: A new molecular dynamics method. *J Appl Phys*. 1981;52(12):7182-7190. doi:10.1063/1.328693
25. Wang J, Ferguson AL. Mesoscale Simulation of Asphaltene Aggregation. *J Phys Chem B*. 2016;120(32):8016-8035. doi:10.1021/acs.jpcb.6b05925
26. Dickie JP, Yen TFu. Macrostructures of the asphaltic fractions by various instrumental methods. *Anal Chem*. 1967;39(14):1847-1852. doi:10.1021/ac50157a057
27. Frigerio F, Molinari D. A multiscale approach to the simulation of asphaltenes. *Comput Theor Chem*. 2011;975(1-3):76-82. doi:10.1016/j.comptc.2011.03.013
28. Kuznicki T, Masliyah JH, Bhattacharjee S. Molecular Dynamics Study of Model Molecules Resembling Asphaltene-Like Structures in Aqueous Organic Solvent Systems. *Energy & Fuels*. 2008;22(4):2379-2389. doi:10.1021/ef800057n